

Optical Pumping of Rubidium

Jonathon Garamella

(Dated: 27 March 2011)

Optical Pumping was used to examine the Zeeman splitting associated with the hyperfine structure of Rubidium. The g -factors, specifically g_f , were found to be 0.48 ± 0.05 and 0.32 ± 0.05 for ^{87}Rb and ^{85}Rb respectively in the low magnetic field strength Zeeman region. These values compare to theoretical values of $1/2$ and $1/3$. From the g_f values, the related nuclear spins, \vec{I} , were found to be 1.58 ± 0.09 and 2.58 ± 0.09 , compared to theoretical values of $3/2$ and $5/2$. The quadratic Zeeman effect was also examined and transitions of RF energy were observed at 4.0 MHz to be between 6.8 and 6.9 gauss. These values were quantitatively compared to theoretical values using the Breit-Rabi equation.

I. INTRODUCTION

The study of quantum mechanics is largely dependent upon electronic and nuclear quantum numbers associated with the angular momentum of the atom. The spin angular momentum (\vec{S}) and orbital angular momentum (\vec{L}) can be combined to fully describe the electron by the total non-nuclear angular momentum (\vec{J}). Clearly, \vec{J} ignores the angular momentum of the nucleus (\vec{I}). Thus, another quantum number, \vec{F} , is used to describe the coupling between the angular momentum of the electron with that of the nucleus such that $\vec{F} = \vec{I} + \vec{J}$. In this way, \vec{F} describes the net angular momentum of the atom. These numbers can be predicted theoretically and determined experimentally. This experiment attempts to determine the nuclear spin for two isotopes of Rubidium, ^{85}Rb and ^{87}Rb .

This experiment hinges upon a process known as optical pumping. To optically pump a population of atoms, EM radiation is used to excite the atoms from a variety of states into one. Stimulated emission of radiation, a electromagnetic property critical to lasers and masers, is investigated by optical pumping. The knowledge of nuclear spin is critical in technologies dependent upon nuclear perturbation, such as Nuclear Magnetic Resonance (NMR) and Magnetic Resonance Imaging (MRI).

This paper will begin by explaining the experimental apparatus and the theory associated with both the low field and quadratic Zeeman splitting followed by a procedural overview with accompanying results. The paper will culminate with a discussion of the property of nuclear spin.

II. THEORY AND APPARATUS

Understanding the apparatus for this experiment is important in order to understand the theory. Many parts of the apparatus are dictated by the theory and vice versa. Therefore, the two will be explained simultaneously. The basic experimental design can be seen in Figure II. Resonant light is emitted from a Rubidium discharge lamp and on its way to the absorption cell passes through an interference filter. This filter removes light

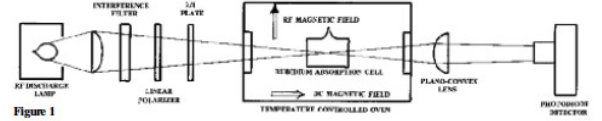


FIG. 1. Diagram of optical pumping experimental set up

emitted at a wavelength of 780 nm as it does not pertain to this experiment and allows light at wavelength of 795 nm to pass through. This light then passes through a linear polarizer and a $1/4$ wave plate which circularly polarizes the light. This light travels to the absorption cell which contains Rubidium atoms and Xenon, an inert gas. The Xenon serves to act as a buffer gas because collisions between excited Rubidium atoms and Xenon atoms are less likely to result in photon emission than collision between the walls. Such collisions would defeat optical pumping, as we will soon see.

The circularly polarized light serves to excite Rubidium atoms from $^2S_{1/2}$ ground state to a $^2P_{1/2}$ level. Since the light is circularly polarized, it only allows $\Delta M = +1$ electric dipole transitions in the atom. In the presence of a weak magnetic field, the degenerate energy levels split into different states as seen in Figure II. The number of states is dependent upon F such that the number of states is equal to $2F + 1$. Thus, the $F=1$ state has 3 M states and $F=2$ has 5. Since the circularly polarized light mandates only $\Delta M = +1$ transitions, the $M = +2$ states in both the $^2S_{1/2}$ ground state and $^2P_{1/2}$ first excited state will become occupied. Spontaneous decay from random collisions is the only way for atoms to change from these $M = +2$ energy levels as there is no $M = +3$ level for the light to force the atom into. The transitions of this decay are defined by $\Delta M = +1, 0, -1$. As light continues to hit the absorption cell, the $M = +2$ sublevel of the ground state will become increasingly populated as opposed to the $M = +2$ of the excited state as all the excited states can decay back into the ground state. If most of the population is in the $M = +2$ state, no light will be absorbed by the Rubidium and it will be transmitted at peak intensity to a photo detector which is hooked up to an oscilloscope beyond the absorption cell. When the intensity measured by the photo detector reads out as a constant peak on the oscilloscope, the system is said to be

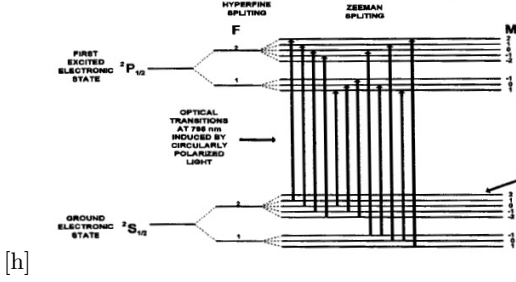


FIG. 2. Energy level diagram of low magnetic field Zeeman splitting in Rubidium

pumped. If a large population exits this state, light will be absorbed by the Rubidium and optical pumping will be defeated, causing a dip to appear on the oscilloscope readout.

The Hamiltonian that describes the perturbation from an external magnetic field on the electronic and nuclear magnetic moments is

$$H = ha\mathbf{I} \cdot \mathbf{J} - \frac{\mu_J}{J} \mathbf{J} \cdot \mathbf{B} - \frac{\mu_I}{I} \mathbf{I} \cdot \mathbf{B}, \quad (1)$$

where μ_J and μ_I are the electronic and nuclear magnetic moment respectively. This accounts for the energy splitting as seen in Figure II. If the interaction of the nucleus is ignored, the energy levels can be solved from Equation 1 to be

$$E = g_J \mu_0 M B, \quad (2)$$

given μ_0 is the bohr magneton ($\mu_0 = 9.27 \times 10^{-24} \text{ J/T}$) and g_J is the Lande g-factor, described by

$$g_J = 1 + \frac{J(J+1) + S(S+1) - L(L+1)}{2J(J+1)}. \quad (3)$$

When the nucleus is considered, a new g-factor emerges as

$$g_F = g_J \frac{F(F+1) + J(J+1) - I(I+1)}{2F(F+1)}. \quad (4)$$

The interaction energy now incorporates g_f and is written as

$$W = g_F \mu_0 M_f B. \quad (5)$$

Equations 5 and 4 will be most important for the purposes of our experiment. It is evident that Equation 5 is linear in terms of B . Thus, if one could create a plot of energy versus magnetic field strength, the slope of a best fit line would simply be $g_F \mu_0 M_f$. From this, g_f can easily be ascertained. Once g_f is found, Equation 4 can be manipulated to discover I , as F and J are already known from the spectroscopic ground state.

Equation 5 is successful when the magnetic field strength is low and the Zeeman splitting is small relative to the hyperfine energy. As the magnetic field and

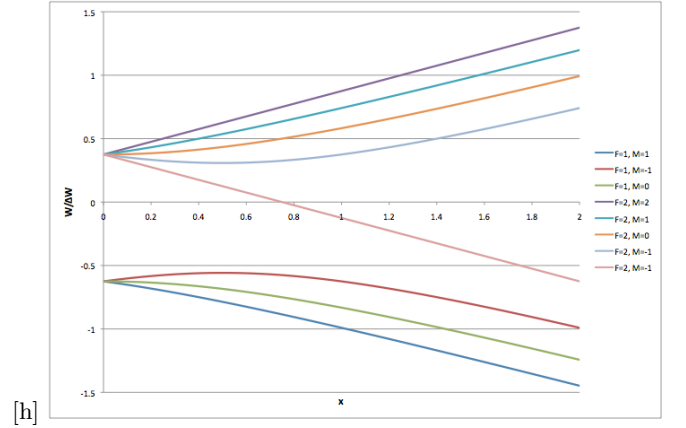


FIG. 3. Simplified model of the Breit-Rabi equation for ^{87}Rb . $W/\Delta W$ is dimensionless and represents the interaction energy and is plotted against the dimensionless number x , which represents the magnitude of the external magnetic field.

interaction energy increase, however, the energy splitting begins to become quadratic as I and J begin to decouple. The Hamiltonian can be diagonalized via perturbation theory to yield

$$W(F, M) = -\frac{\Delta W}{2(2I+1)} - \frac{\mu_I}{I} B M \pm \frac{\Delta W}{2} \left[1 + \frac{4M}{2I+1} x + x^2 \right]^{1/2}, \quad (6)$$

where

$$x = (g_J - g_I) \frac{\mu_0 B}{\Delta W} \quad \text{and} \quad g_I = -\frac{\mu_I}{I \mu_N}. \quad (7)$$

Equation 6 is known as the Breit-Rabi equation. A simplified version modeled after ^{87}Rb can be seen in Figure 6. This was the theoretical model to which the experimental magnetic field values were compared for the quadratic Zeeman portion of the experiment. When x is very small (very small magnitude of B) the graph is said to be in the Zeeman region, where the energy levels are linear in B . As x increases, the graph enters the quadratic region. This is where I and J begin to decouple and M is no longer a “good” quantum number. As x continues to increase, the lines again become linear in what is known as the Paschen-Back region. This is when I and J are entirely decoupled. Our experiment will focus on the non-linear intermediate zone.

The net external magnetic field in this experiment is controlled by three sets of Helmholtz coils. The magnetic field of the earth is also a factor, though it cannot be controlled so much as manipulated. Two of the Helmholtz coil sets, one oriented vertically and another horizontally, are static coils and are used to cancel out unwanted external magnetism. The third coil is also oriented horizontally, though it can be adjusted to sweep through a desired magnetic magnitude. As such, it is known as the sweep coil.

RF radiation is used to stimulate emission for both the low field and quadratic Zeeman experiments. Since

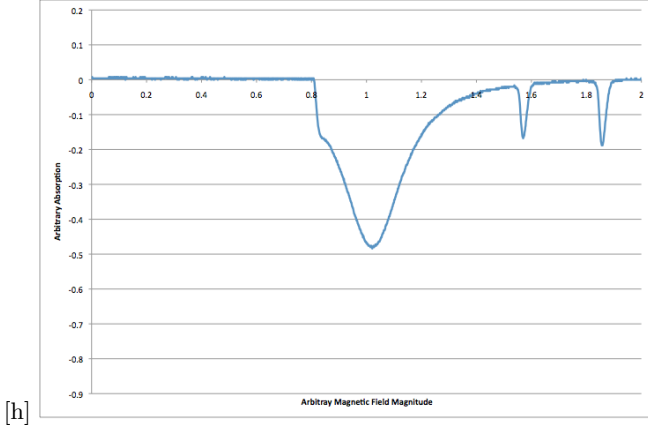


FIG. 4. Absorption versus magnetic field strength for at 71 kHz. From left to right is the zero field resonance followed by RF absorption for ^{87}Rb and ^{85}Rb .

an optically pumped system will output a constant maximum on the oscilloscope, RF radiation from a variable source is used to defeat optical pumping and cause dips to appear on the oscilloscope as less light is transmitted. The RF radiation does this by providing energy to the atoms which can be used to degrade into a different M level.

III. EXPERIMENT AND RESULTS

A. Zero Field Calibration

Before the low field or quadratic Zeeman effects could be investigated, the apparatus had to be calibrated in order to ensure that the measured applied magnetic field was not corrupted by that of the earth or other sources. To do this, the apparatus was aligned so that it was oriented along with a component of earth's magnetic field. The sweep coils were then used to find the zero field resonance of the optical radiation. The voltage at this zero field resonance was measured across a one ohm resistor. This gives a one to one relationship to the current given $V = IR$. The magnitude of the magnetic field is given by

$$B(\text{gauss}) = 8.991 \times 10^{-3} IN/R, \quad (8)$$

where I is the current in amps, N is the number of turns, and R is the radius. For the sweep field, $N = 11$ and $R = 0.1639$ m. Using Equation 8, the residual field was found to be 0.189 gauss. This value was subtracted from all low field Zeeman measurements. Figure III A shows an oscilloscope output for a zero field resonance at 71 kHz.

B. Low Field Zeeman Splitting

RF radiation was applied to the system to cause transitions between the Zeeman levels in the presence of a small magnetic field. The radiation ranged from 40-65 kHz in increments of 5 kHz. Voltages were obtained for each frequency at the minimum of each peak for both ^{87}Rb and ^{85}Rb . These were converted into magnetic field magnitudes in the same manner as the sweep field calibration, using Equation 8. As seen in Figure IIIB, graphs of frequency versus magnetic field strength were created and g_f obtained from the slope of the best fit line. The val-

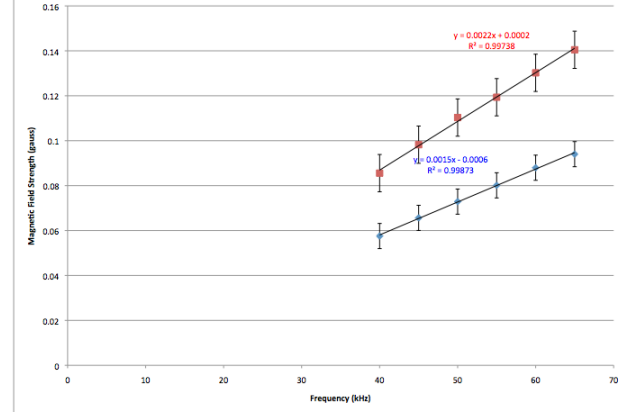


FIG. 5. Frequency versus magnetic field for Rubidium isotopes. On the graph, ^{87}Rb is represented in blue and ^{85}Rb in red.

ues for g_f found from the trendlines were 0.48 ± 0.05 and 0.32 ± 0.05 for ^{87}Rb and ^{85}Rb respectively. These compare to theoretical values of $1/2$ and $1/3$. From these values, the nuclear spins of each isotope were found to be 1.58 ± 0.09 and 2.58 ± 0.09 . Quantum theory demands the nuclear spin be quantized in $1/2$ integer values. The closest value for ^{87}Rb is $3/2$ and for ^{85}Rb is $5/2$. These compare well to theoretical values of $3/2$ and $5/2$ for ^{87}Rb and ^{85}Rb respectively. The error associated with the measurements is a result of the reading taken from the oscilloscope. The value changed continuously and it was not possible to measure the voltage with exact precision.

C. Quadratic Zeeman Effect

RF radiation at a frequency of 4.0 MHz was used to stimulate energy transitions in ^{87}Rb in the quadratic Zeeman regime. There are six dips in Figure IIIC as only six of the seven energy level transitions can be reached by 4.0 mHz radiation; the energy gap between the $F=2$ $M=-2$ to $F=1$ $M=-1$ is too large.

Figure IIIC is a comparison between the energy transitions seen experimentally and those predicted by the Breit-Rabi equation. The experimental values seem very high relative to the theoretical values though the gaps

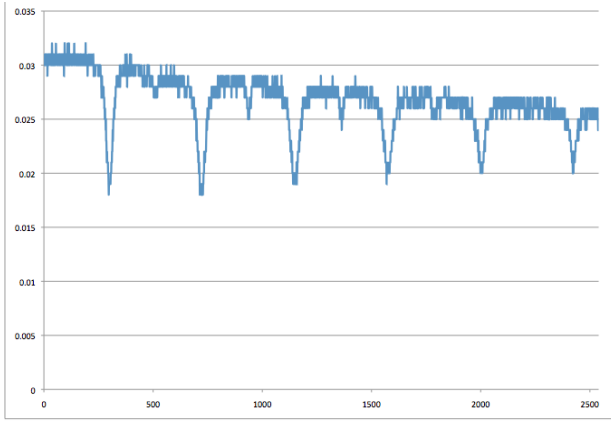


FIG. 6. Arbitrary absorption versus magnetic field strength. The six dips correspond to the six energy transitions attainable at 4.0 MHz

between the states is similar in both cases. It is also uncertain why some theoretical values match when none of the experimental values are the same. It is perhaps a result of an oversimplification of the Breit-Rabi equation itself, suggesting flaws with the theoretical values.

Expected Transtion	Experimental B Field (gauss)	Theoretical B Field (gauss)
F=1, M=-1 to 0	6.918 ± 0.5	5.8054
F=1, M=0 to 1	6.895 ± 0.5	5.8128
F=2, M=2 to 1	6.871 ± 0.5	5.8201
F=2, M=1 to 0	6.849 ± 0.5	5.8128
F=2, M=0 to -1	6.827 ± 0.5	5.8054
F=2, M=-1 to -2	6.805 ± 0.5	5.7981

FIG. 7. A comparison for experimental values and those obtained theoretically via the Breit-Rabi equation.

IV. CONCLUSION

The values for g_f were found to be 0.48 ± 0.05 and 0.32 ± 0.05 for ^{87}Rb and ^{85}Rb respectively in the low B field Zeeman region. The corresponding values for nuclear spin, I , were found to be 1.58 ± 0.09 and 2.58 ± 0.09 for ^{87}Rb and ^{85}Rb respectively. These values compare to theoretical values of $5/2$ and $3/2$. The quadratic Zeeman effect was also analyzed for ^{87}Rb at 4.0 MHz and transitions were seen between 6.8 and 6.9 gauss. These values do not match theoretical values, though it is uncertain why this is.